April 15, 2005

ANALYSIS OF DEPRESSURIZATION ACCIDENT FOR A 2400 MW GAS COOLED REACTOR - EFFECTS OF THE REACTOR CAVITY COOLING SYSTEM

Interim Report on GFR System Design and Safety

Lap-Yan Cheng
Hans Ludewig

Submitted to DOE GEN-IV Program
by
Brookhaven National Laboratory

1.0 INTRODUCTION

The ATHENA analysis presented here examines the effects of the reactor cavity cooling system (RCCS) on decay heat removal for a gas cooled reactor during a depressurization accident. The new analysis is an extension of a previous study [1] that assessed the performance of decay heat removal by natural circulation cooling under depressurization accident conditions for a helium cooled reactor. In the previous analysis passive decay heat removal is enabled by an emergency cooling system (ECS) that directs, by natural circulation, the hot helium gas from the reactor to an ex-vessel heat exchanger. A dominant factor in determining the effectiveness of natural circulation cooling is the system pressure. A higher pressure results in a denser gas and that leads to a higher buoyancy head and subsequently a higher flow rate. In a depressurization accident initiated by a component breach, the pressures of the reactor vessel and the guard containment will converge to an intermediate value. The impact of this common pressure on the maximum fuel temperature has been evaluated parametrically in the previous study. In that analysis, different common pressures (system back pressure) were obtained by varying the free volume of the guard containment. An alternate means of decay heat removal is the RCCS that surrounds the reactor vessel. Core decay heat is transferred to the reactor vessel by conduction and radiation and the RCCS absorbs the thermal energy from the reactor vessel directly by radiation and indirectly from the guard containment atmosphere by convection. The impact of the RCCS on the guard containment atmosphere and the maximum fuel temperature is the subject of the present study.

2.0 ATHENA/RELAP5 Model

In the current analysis, heat structures and hydraulic volumes are added to represent the RCCS and the new system replaces the heat structure in the previous model that represented the reactor vessel support structure. The heat structures used in the ATHENA model for convective and radiative heat transfer are shown in Figure 1.

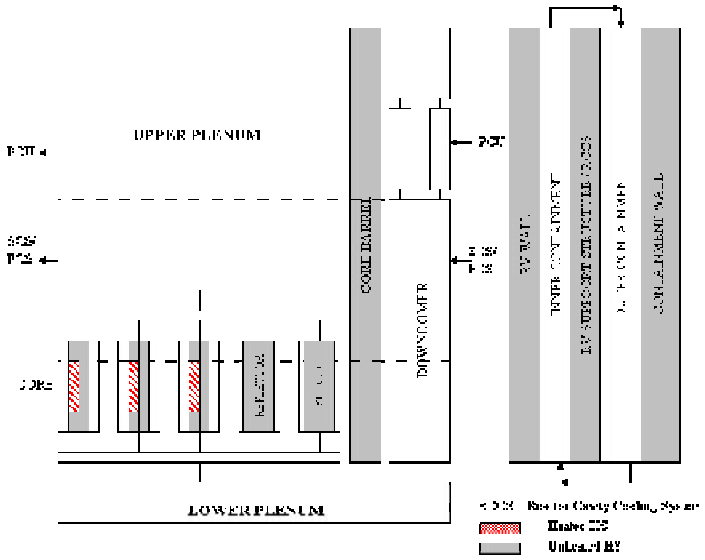

Figure 1 – Reactor Vessel and Guard Containment Heat Structures.

The heated heat structures (HS), i.e. the fuel pins, identified in Figure 1 are the source of energy and the unheated heat structures are other components that participate in the exchange of thermal energy by radiation. In the previous analysis [1] the zone of influence of radiative heat transfer is assumed to be confined to the cylindrical section that coincides with the vertical extent of the fueled region of the core. As an example, even though the core barrel (also, the reactor vessel wall, and the reactor vessel support structure) extends to the upper plenum, only the lower portion between the lower and upper boundaries of the fueled zone (1.347m in height) participates in radiative heat transfer. This assumption is relaxed in the current analysis to accommodate the RCCS that spans the entire height of the reactor vessel. In particular the entire core barrel now communicates radiatively with the full height of the reactor vessel wall and in turn the full height of the reactor vessel radiates to either the vessel support structure (old configuration) or the RCCS (new configuration).

The ATHENA model for the RCCS is based on a set of input developed at INL [2]. As shown in Figure 2 the RCCS is modeled with three cylindrical heat structures that are

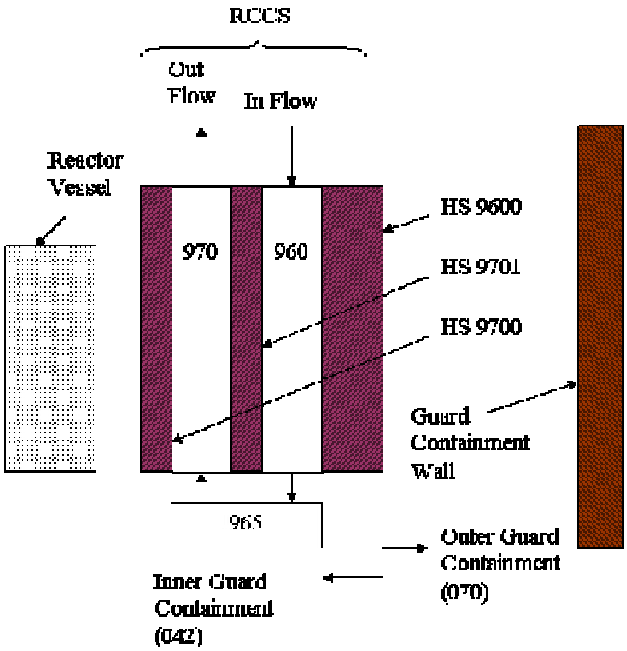

Figure 2 - ATHENA Model of the RCCS

concentric with the reactor vessel. The inner wall (HS 9700), closest to the reactor vessel is followed by the interior wall (HS 9701) and the outer wall (HS 9600) respectively. The incoming (down flow) and outgoing (up flow) streams of cooling water are separated by the interior wall. The inner wall is made of stainless steel and has a wall thickness of 0.0127m. This wall is in contact with the inner guard containment volume (042) that occupies the part of the guard containment that is within the confine of the RCCS and also includes the region above the reactor and the RCCS. The interior wall of the RCCS is modeled with a 0.01746m-thick structure of low conductivity material. The outer wall

of the RCCS has two layers, a 0.0127m layer of stainless steel and a 1m thick wall of concrete. The concrete wall is in contact with the atmosphere of the outer guard containment volume (070). The inner and outer guard containment volumes are connected at the top and bottom to facilitate internal recirculation. The wall of the 44m high guard containment is modeled with a 0.02m thick concrete wall.

It is assumed in the ATHENA calculations that the outside surface of the guard containment wall is kept at a constant temperature of 30°C by a thermal management system embedded in the wall. The RCCS is assumed to be cooled by 30°C water and the flow is high enough to maintain the temperature rise to less than 1 deg. C. These two boundary conditions are set to maximize the cooling of the guard containment atmosphere by the containment wall and the RCCS.

3.0 ATHENA TRANSIENT ANALYSIS

The new analysis with the addition of the RCCS is performed by using the same system model and the same depressurization accident as described in Ref [1]. With the modifications to the radiative heat transfer model for the core barrel, vessel wall, and vessel support structure, it becomes necessary to establish a new baseline analysis for use in comparison with the case of the RCCS. The new baseline case is similar to Case 4 described in Ref [1]. The depressurization accident is initiated by a 0.00645 m^2 (1.0 in^2) rupture in the cold leg of one of the PCUs (4 loops of 600MW each). A guard containment free volume of 20250 m^3 is assumed and the initial pressure and temperature of the guard containment atmosphere are one atmosphere and 30°C respectively.

3.1 Transient Cases

Two transient cases have been run, one with and one without the RCCS. The later is the new base case. The benefits of having the RCCS are evident in the guard containment conditions. Both the pressure and temperature of the guard containment are lower in the case with RCCS (Case 5) than the case without (Case 4a, the base case) it. The trend of lower temperature however does not extend to the peak fuel temperature. Results of the two cases, at the end of a 24000s run, are summarized below.

Case Identification	Final Peak Fuel Temperature (K)	Final Containment Pressure (MPa)	Final Containment Temperature (K)
Case 4a (No RCCS, Base Case)	1594	0.658	355.
Case 5 (With RCCS)	1772	0.611	325.

It is noted that the maximum fuel temperature during the depressurization accident is only a few degrees different from the final peak fuel temperature shown in the above table. With a lower guard containment pressure, the natural circulation flow established

in the reactor is correspondingly lower in the case with RCCS. This then leads to a higher peak fuel temperature in Case 5. The peak fuel temperature result demonstrates that the predominant mode of decay heat removal is by convection while radiative heat transfer only serves a minor role in heat dissipation from the fuel. For the purpose of comparison, at the initial steady-state reactor power of 2400MW, the RCCS removes about 2MW of power while the emergency cooling system (ECS) removes about 20MW of power from the reactor at the end of the calculation at 24000s.

It is noted that although Case 4a is the same transient as Case 4 in Ref. [1], the new analysis has a few modifications in the inputs for the heat structures. These changes resulted in a generally lower guard containment pressure and lower temperatures (fuel and guard containment) than before.

3.2 Analysis of Transient Results

The progression of the depressurization transient for the two cases is very similar and the transient results for both cases are plotted together to facilitate comparison of trends.

3.2.1 Heat Removal Rate of the Emergency Cooling System

Plotted in Figure 3 is the rate of heat transfer into the water side of the HEATRIC heat exchanger in the emergency cooling system. The reactor power also is shown in the figure for comparison. The initial surge in the heat removal rate is due to the hydraulic transient on the water side of the heat exchanger as explained in Ref. 1. A comparison between Figures 3, 4 and 5 shows that as the reactor pressure comes into equilibrium with the guard containment pressure, indicating an end to the depressurization phase of the transient, there is a slow migration of the heat exchanger heat removal rate towards the reactor power. This trend is indicative of the approach to a quasi-steady state where the natural circulation heat removal rate matches that of the reactor power.

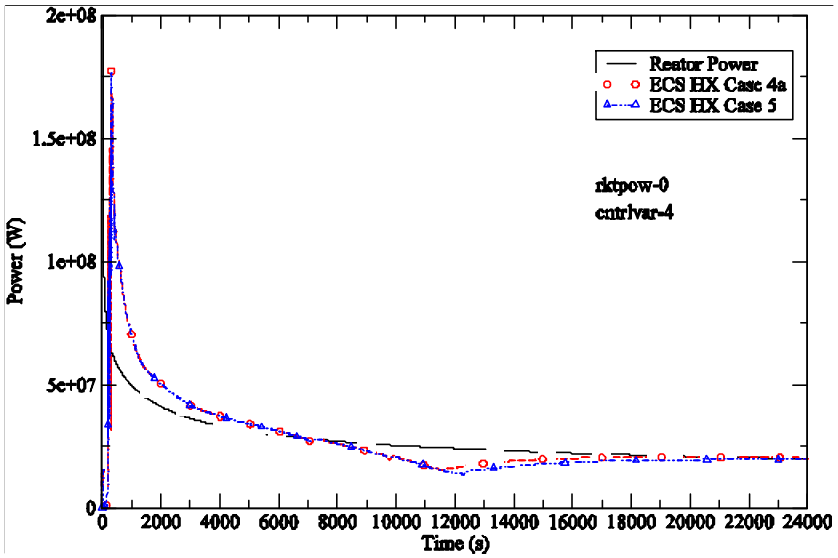

Figure 3 – Reactor Power and Emergency Heat Exchanger Heat Removal Rate.

3.2.2 Reactor Pressure

The pressure of the reactor upper plenum is shown in Figure 4. With the initiation of the break at time zero, the current RELAP5/ATHENA model assumes a linear coast down of the velocity of the flow from the power conversion unit (PCU) to the reactor. This is an interim scheme to simulate the behavior of a tripped PCU until a compressor/turbine model is developed for a more realistic representation of the PCU. The mean initial pressure of the PCU is less than the reactor pressure. With no rotating machinery in the current model to provide hydraulic head in the PCU, helium gas in the reactor quickly depressurizes into
the PCU volumes. This results in a rapid drop in reactor pressure at time zero. The rest of the depressurization is more gradual and is due to leakage through the break into the guard containment. For much of the depressurization transient the helium flow through the leak is choked and thus both cases have similar reactor pressure until the point at which the reactor pressure equalizes with the guard containment pressure. It is noted that the blow down takes a little longer in Case 5 than Case 4a. The reason is a lower back pressure in the latter (see Figure 5).

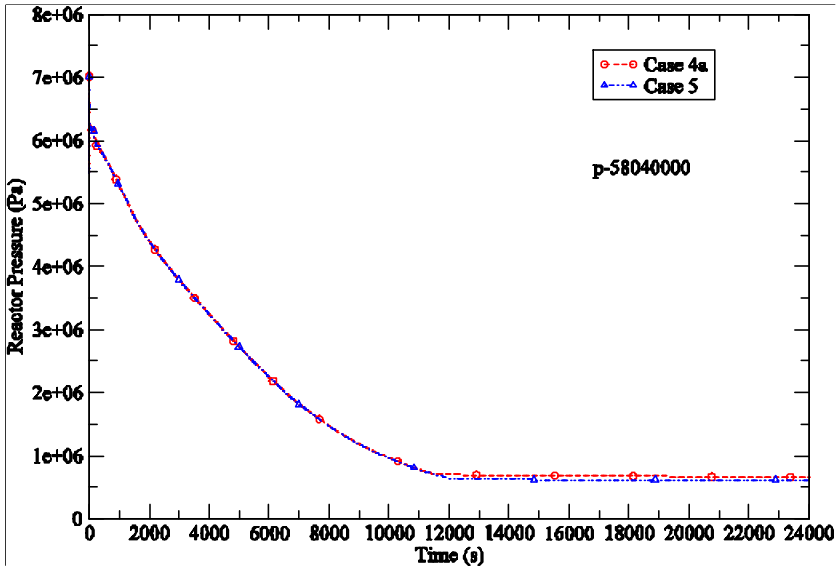

Figure 4 – Reactor Pressure in the Upper Plenum.

3.2.3 Guard Containment Pressure

There are several factors that determine the pressure build up in the guard containment after a leak in the reactor primary circuit. They are:

1. Initial state of the guard containment atmosphere, i.e. temperature, pressure, and volume.
2. Presence of heat structure to absorb sensible heat inside the guard containment.
3. Presence of active cooling device in the guard containment.

4. Through wall heat transfer to the outside.
5. Energy and mass transfer through the leak into the guard containment.

In Figure 5 the rate of pressure build up is seen to be faster for Case 4a than Case 5 and the former also has a higher containment pressure. A peak pressure is reached when the reactor and guard containment have reached the same pressure and the combined heat removal from the Emergency Cooling System, Reactor Cavity Cooling System, and heat conduction through the guard containment wall exceeds the decay power.

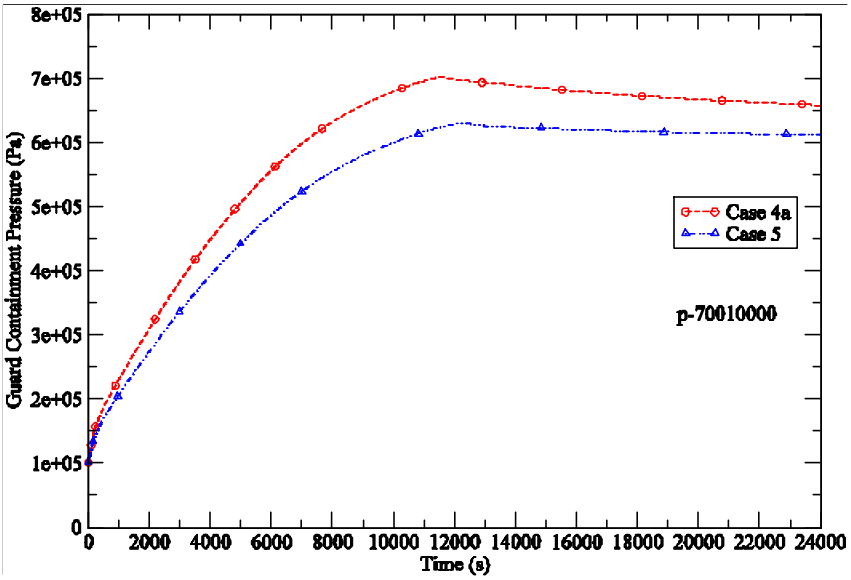

Figure 5 – Guard Containment Pressure.

3.2.4 Guard Containment Gas Temperature

The gas temperature of the guard containment increases rapidly after the initiation of the depressurization accident because of the relatively low heat capacity of its atmosphere. Figure 6 shows that the gas temperature is lower when the RCCS is included in the analysis. A high gas temperature is of concern not only for the environmental qualification of equipment and instruments inside the guard containment but also for the structural integrity of the support structures and the guard containment itself.

3.2.5 Peak Fuel Temperature

Figure 7 shows the peak fuel temperature as a function of time. It is obtained from the RELAP5/ATHENA results by defining a control variable that searches for the maximum temperature for all fuel heat structures at all axial locations. It is noted that there is little deviation between the peak fuel temperatures for the two cases until about 12000s

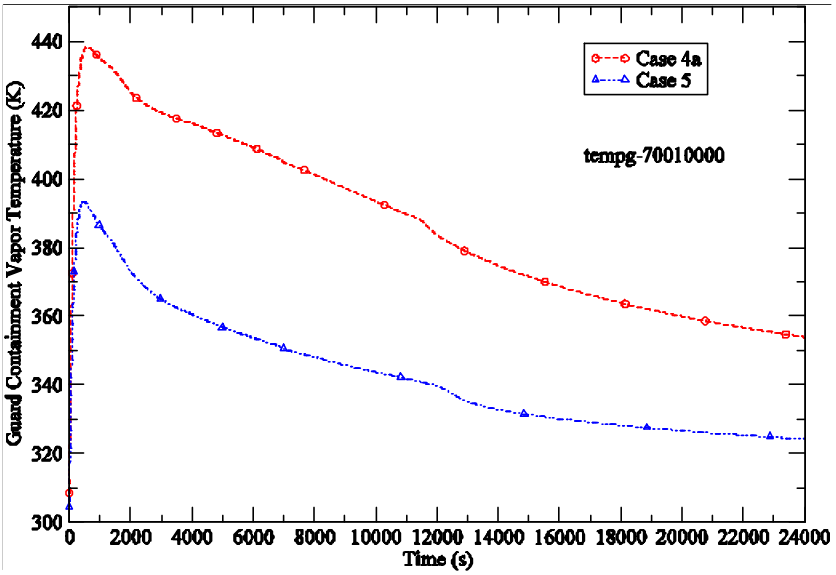

Figure 6 – Gas Temperature Inside the Guard Containment.

when Case 4 has finished its blow down. Before that time the two cases have the same reactor pressure and almost the same natural circulation flow (see Figure 8). In both cases the maximum fuel temperature during the transient is within the success criterion of 1873K, with the RCCS case (Case 5) exhibiting a closer approach to the limit.

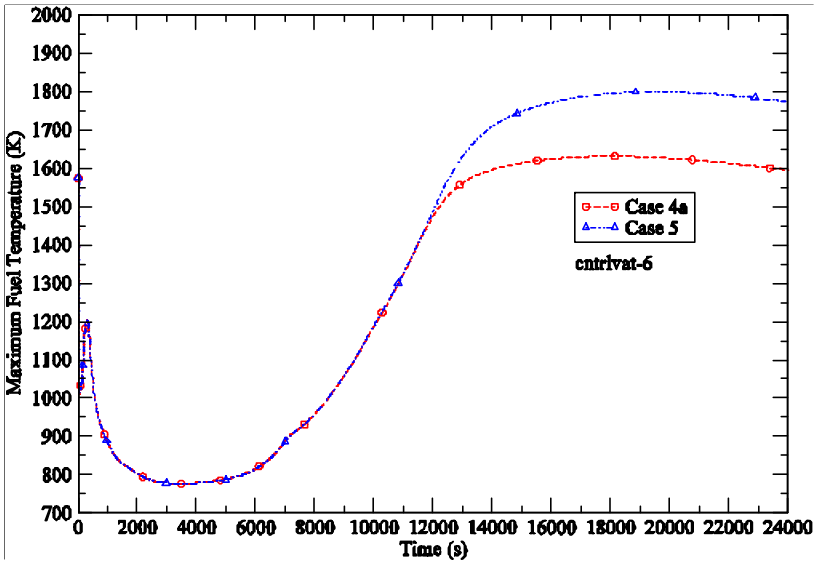

Figure 7 – Peak Fuel Temperature Core-wide.

3.2.6 Helium Flow in Natural Circulation

Natural circulation flow is established when the pressure difference across the check valve in the emergency heat exchanger loop has reached a threshold value. The helium flow rate shown in Figure 8 clearly demonstrates its dependence on the reactor pressure (see Figure 4). Higher flow rates are achieved at higher pressures and that is the reason the base case has a higher flow rate than the RCCS case when the system pressure has reached its quasi-steady state value. Based on economic and engineering constraints a maximum design pressure will be specified for the guard containment and that will have a direct bearing on the maximum passive heat removal rate achievable by natural circulation alone.

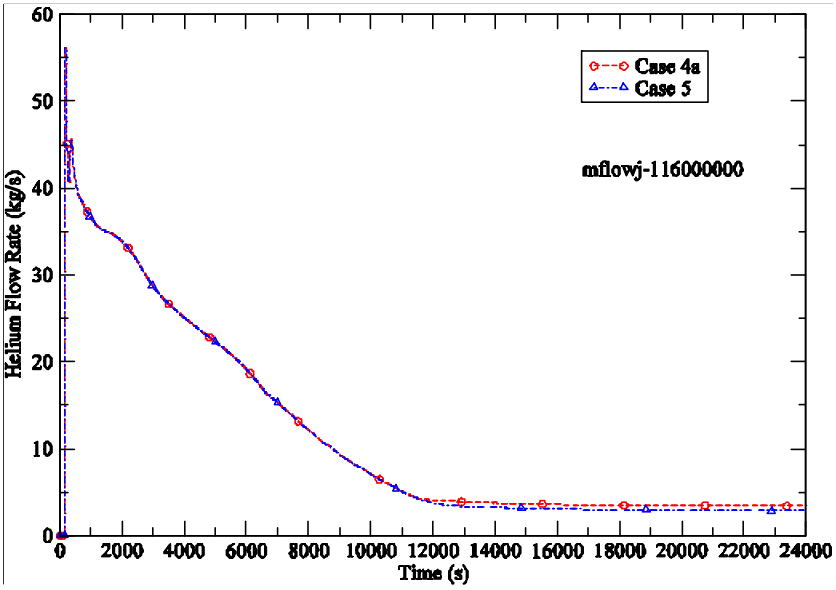

Figure 8 – Natural circulation flow rate of helium gas.

3.2.7 Gas Temperature at Core Outlet

The gas temperature at the core outlet, shown in Figure 9, generally reflects the rate of heat transfer from the core to the helium flow. The progression of the core outlet temperature thus follows the trend of the fuel temperature shown in Figure 7.

3.2.8 Gas Temperature at Core Inlet

The initial surge in the core inlet temperature, shown in Figure 10, is somewhat unrealistic and is due to an approximation in the current PCU model discussed earlier in relation to the reactor pressure. In general the trend of the core inlet temperature corresponds to the difference between the heat removal rate of the emergency heat exchanger and reactor power. A positive differential implies a decrease in core inlet temperature and vice versa. The core inlet temperature is very similar for both cases and the general trend follows the ECS heat exchanger heat removal rate shown in Figure 3.

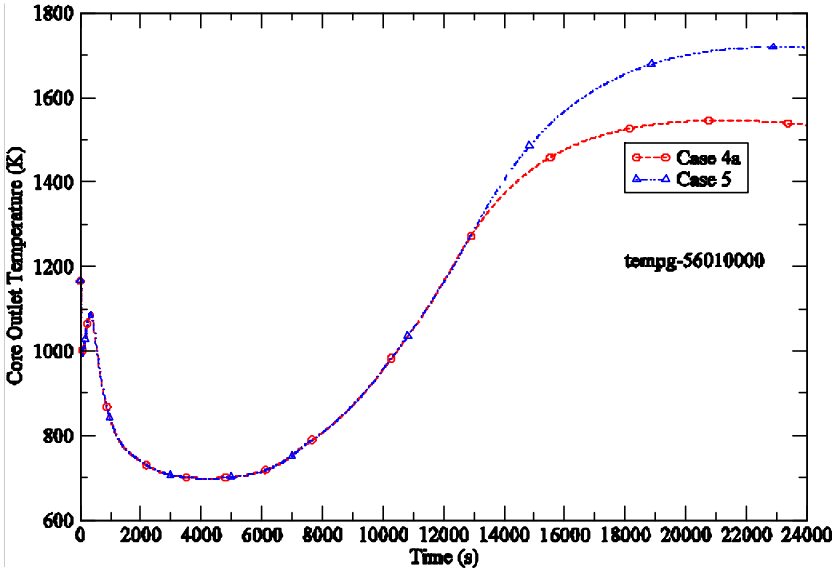

Figure 9 – Gas temperature at core outlet.

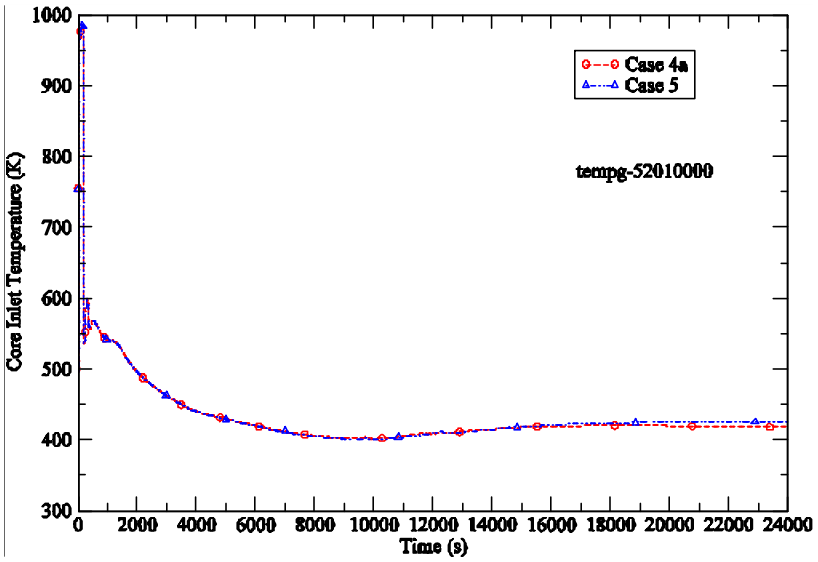

Figure 10 – Gas temperature at core inlet.

4.0 SUMMARY and CONCLUSIONS

The analysis presented here is an extension of a previous study [1] of a depressurization transient for a 2400MW gas cooled reactor with a passive decay heat removal scheme based on natural circulation cooling. The new analysis includes the effects of a Reactor Cavity Cooling System that surrounds the reactor. The analysis shows that while the RCCS is good for lowering the guard containment pressure and temperature, its presence

has a negative impact on the peak fuel temperature because the lower back pressure also reduces the natural circulation flow that removes most of the decay heat by convection. While the RCCS may be beneficial for other non-LOCA type accidents its use in a depressurization accident would require further studies to evaluate the trade-offs. The same observation applies to other active or passive means of cooling the guard containment atmosphere. One example is the heat loss through the guard containment wall. Internal flow inside the guard containment tends to be quite complex and to correctly model the loss of heat by convection to the wall would require a more detailed analysis than what is possible with a system code. The capability to accommodate other break sizes should also be evaluated in the design of the guard containment. It is also recognized that the accident analysis will not be complete without the power conversion unit being properly modeled.

5.0 REFERENCES

[1] Cheng, L., Ludewig, H. and Jo, J., "Passive Decay Heat Removal for a 2400 MW Pin Core by Natural Circulation," BNL report submitted to the DOE GEN-IV Program, January 2005.

[2] Davis, C., Personal communication with L. Cheng (Electronic files related to major improvements made to the RELAP5-3D/ATHENA computer code for analysis of the GFR as part of an annual report (2004) for an INL LDRD), April 7, 2005.